

# Doubly charmed baryon production in heavy ion collisions

Xiaojun Yao\* and Berndt Müller†

*Department of Physics, Duke University, Durham, NC 27708, USA*

(Dated: December 14, 2024)

We give an estimate of  $\Xi_{cc}^{++}$  production rate and transverse momentum spectra in relativistic heavy ion collisions. We use Boltzmann transport equations to describe the dynamical evolution of charm quarks and diquarks inside quark-gluon plasma. In-medium formation and dissociation rates of charm diquarks are calculated from potential non-relativistic QCD for the diquark sector. We solve the transport equations by Monte Carlo simulations. For 2.76 TeV Pb-Pb collisions with 0 – 10% centrality, the number of  $\Xi_{cc}^{++}$  in the transverse momentum range 0 – 5 GeV and rapidity from –1 to 1 is roughly 0.026 per collision. We repeat the calculation with a melting temperature 250 MeV above which no diquarks can be formed. The number of  $\Xi_{cc}^{++}$  produced in the same kinematic region is about 0.016 per collision.

Recently the LHCb collaboration reported the discovery of a doubly charmed baryon carrying two units of positive charge,  $\Xi_{cc}^{++}$ , with a mass  $m(\Xi_{cc}) \approx 3621$  MeV [1]. The particle is stable under strong interactions and only decays weakly. The structure of  $\Xi_{cc}^{++}$  can be thought of as an up quark bound around a deeply bound state (diquark) of two charm quarks [2]. Just as a pair of heavy quark and heavy anti-quark attract each other and can form a bound state in the color singlet channel, a pair of two heavy quarks also attract and can form a bound state, a heavy diquark, in the anti-triplet representation.

The peculiar properties of  $\Xi_{cc}^{++}$  have stimulated new theoretical and experimental research. Here we consider the production of  $\Xi_{cc}^{++}$  in high energy heavy ion collisions, where a hot nuclear environment, the quark-gluon plasma (QGP), is produced. Heavy ion collisions have two advantages in  $\Xi_{cc}^{++}$  production: First, more charm quarks are produced in a single collision. Second, the deconfined QGP medium lasts roughly 10 fm/c, during which time the charm quarks can diffuse in the QGP via interactions with light quarks and gluons. If two independently produced charm quarks come together as a result of this diffusion, they can combine into a charm diquark bound state if the temperature of the QGP is not too high.

After its formation the charm diquark also diffuses in the QGP because it carries color charge. At the same time, the charm diquark may dissociate by absorbing a real or virtual gluon. So the whole process is a dynamical in-medium evolution involving charm diquark formation, diffusion and dissociation. This is similar to the in-medium evolution of heavy quarkonia, such as the  $J/\psi$ , except that the heavy diquarks carry color while the quarkonia are color neutral. At the transition from the deconfined QGP phase to the hadronic phase, the charm diquarks hadronize into doubly charmed baryons by absorbing an up or down quark from the medium.

We will describe the in-medium dynamical evolution of charm quarks and diquarks by a set of coupled Boltzmann equations. By connecting the transport equations with the initial production of charmed quarks from the hard collision and the hydrodynamical background, we

obtain an estimate of the yield and  $p_T$ -spectrum of  $\Xi_{cc}^{++}$  in Pb-Pb collisions at 2.76 TeV. Finally, we study the static screening effect of the QGP on the production process.

The set of coupled Boltzmann transport equations for the charm quark and diquark distribution functions  $f(\mathbf{x}, \mathbf{p}, t)$  is given by

$$\begin{aligned} \left(\frac{\partial}{\partial t} + \dot{\mathbf{x}} \cdot \nabla_{\mathbf{x}}\right) f_c(\mathbf{x}, \mathbf{p}, t) &= \mathcal{C}_c - \mathcal{C}_+ + \mathcal{C}_- \\ \left(\frac{\partial}{\partial t} + \dot{\mathbf{x}} \cdot \nabla_{\mathbf{x}}\right) f_{cc}(\mathbf{x}, \mathbf{p}, t) &= \mathcal{C}_{cc} + \mathcal{C}_+ - \mathcal{C}_-. \end{aligned} \quad (1)$$

Here we will focus on the ground charm diquark state  $cc(1S)$  because excited states are loosely bound and cannot survive at high temperature. In the following, by charm diquark we mean the  $cc(1S)$  state. The collision terms  $\mathcal{C}_c$  and  $\mathcal{C}_{cc}$  describe their scattering with thermal constituents of QGP. This process has been described as two-body scattering in the framework of the linearized Boltzmann equation [3–5]. Here we use the elastic scattering rate calculated and implemented in Ref. [6] to describe the in-medium diffusion. The diquark gain term  $\mathcal{C}_+$  is from the combination of a charm quark pair by gluon emission and the loss term  $\mathcal{C}_-$  is from dissociation by gluon absorption.

We calculate the diquark formation and dissociation rates in QGP to the lowest order in potential non-relativistic QCD (pNRQCD) for the diquark sector [7, 8]. The effective field theory can be derived from QCD under the hierarchy of scales  $M \gg Mv \gg Mv^2, T, m_D$  where  $M = 1.3$  GeV is the charm quark mass,  $v \sim 0.4$  is the relative velocity of  $cc$  inside the diquark,  $T$  is the QGP temperature, and  $m_D$  is the Debye screening mass. If  $T$  or  $m_D$  scales as  $Mv$ , the Debye static screening of the color attraction is so strong that no diquark bound states can be formed inside QGP. So the above hierarchy of scales is relevant to diquark formation. The pNRQCD is a systematic expansion in  $v$  or  $1/M$  (NR expansion) and  $r$ , the relative distance between the diquark (multipole expansion). Its Lagrangian is given by:

$$\mathcal{L}_{\text{pNRQCD}} = \int d^3r \text{Tr} \left\{ T^\dagger (iD_0 - H_T) T + \Sigma^\dagger (iD_0 - H_\Sigma) \Sigma + T^\dagger \mathbf{r} \cdot g \mathbf{E} \Sigma + \Sigma^\dagger \mathbf{r} \cdot g \mathbf{E} T \right\} + \dots, \quad (2)$$

where higher order interaction terms in  $1/M$  and  $r$  are omitted, such as interactions between anti-triplets. The Lagrangian of light quarks and gluons is just QCD with momenta  $k \lesssim Mv$ . The degrees of freedom are the anti-triplet  $T(\mathbf{R}, \mathbf{r}, t)$  and sextet  $\Sigma(\mathbf{R}, \mathbf{r}, t)$  where  $\mathbf{R}$  denotes the center-of-mass (c.m.) position and  $\mathbf{r}$  the relative coordinate. They are defined as

$$T = t^l T^l \quad \Sigma = \sigma^\nu \Sigma^\nu, \quad (3)$$

where the  $T^l$  and  $\Sigma^\nu$  are anti-triplet and sextet diquark fields while the  $t^l$  and  $\sigma^\nu$  are the generators of the corresponding representations. They are given by

$$t_{ij}^l = \frac{1}{\sqrt{2}} \epsilon_{ijl} \quad (4)$$

$$\sigma_{11}^1 = \sigma_{22}^4 = \sigma_{33}^6 = 1 \quad (5)$$

$$\sigma_{12}^2 = \sigma_{21}^2 = \sigma_{13}^3 = \sigma_{31}^3 = \sigma_{23}^5 = \sigma_{32}^5 = \frac{1}{\sqrt{2}}. \quad (6)$$

The equations of motion of the anti-triplet and sextet are Schrödinger equations with the Hamiltonians expanded in powers of  $1/M$

$$H_{T,\Sigma} = -\frac{\mathbf{D}_{\mathbf{R}}^2}{4M} - \frac{\nabla_{\mathbf{r}}^2}{M} + V_{T,\Sigma}^{(0)} + \frac{V_{T,\Sigma}^{(1)}}{M} + \frac{V_{T,\Sigma}^{(2)}}{M^2} + \dots \quad (7)$$

where  $\mathbf{D}_{\mathbf{R}}$  is the covariant derivative associated with the c.m. position.

By the virial theorem,  $-\nabla_{\mathbf{r}}^2/M \sim V_{T,\Sigma}^{(0)}$ . So the order of the relative kinetic term is accounted as  $1/M^0$ , not suppressed. The c.m. kinetic term is suppressed because momenta  $k \sim Mv$  have been integrated out in the construction and then  $\mathbf{D}_{\mathbf{R}} \ll Mv$ . Higher-order terms of potentials are also suppressed by  $1/M$  which include relativistic corrections, spin-orbital and spin-spin interactions. We only work to order  $1/M^0$  since the charm quark mass is large. At this order, the Hamiltonians only contain the relative kinetic term and  $V_{T,\Sigma}^{(0)}$ . Inside the deconfined QGP, the potential is flattened and can be approximated by Coulomb interactions

$$V_T^{(0)} = -\frac{2}{3} \frac{\alpha_s}{r} \quad V_\Sigma^{(0)} = \frac{1}{3} \frac{\alpha_s}{r}. \quad (8)$$

The interaction vertex between the anti-triplet and the sextet is a color dipole interaction with the chromoelectric field given by

$$\mathbf{E} = t_F^a \mathbf{E}^a, \quad (9)$$

where  $t_F^a$  is the generator of the fundamental representation.

At leading order in  $r$ , the transition between unbound charm quark pairs and bound diquarks can only occur between an unbound sextet and a bound anti-triplet. The Feynman diagram of the transition via gluon absorption or emission is shown in Fig. 1. For simplicity, we only consider the interaction with on-shell gluons in the QGP. Transitions caused by virtual gluons (inelastic scattering with medium constituents) are at next order in  $\alpha_s$  and neglected here. The scattering amplitude is given by

$$\mathcal{T}_\lambda^{\nu la} = (2\pi)^4 \delta^3(\mathbf{k}_1 + \mathbf{q} - \mathbf{k}_2) \delta(\Delta E) \mathcal{M}_\lambda^{\nu la} \quad (10)$$

$$\mathcal{M}_\lambda^{\nu la} = -igq \text{Tr}(\sigma^\nu t_F^a t^l) (\epsilon_\lambda^*)^i \langle \psi_{1S} | r_i | \Psi_{\mathbf{p}_{\text{rel}}} \rangle \quad (11)$$

$$\Delta E = \frac{k_1^2}{4M} + E_{1S} + q - \frac{k_2^2}{4M} - \frac{p_{\text{rel}}^2}{M}, \quad (12)$$

where  $\mathbf{k}_{1,2}$  are the c.m. momenta,  $\mathbf{p}_{\text{rel}}$  is the relative momentum between the unbound quark pair and  $q = |\mathbf{q}|$  is the gluon energy. In the matrix element,  $|\psi_{1S}\rangle$  is the hydrogen-like  $1S$  wave function for the bound diquark in the anti-triplet, and  $|\Psi_{\mathbf{p}_{\text{rel}}}\rangle$  is the Coulomb wave function for the unbound sextet. The  $1S$  binding energy is given by  $E_{1S} = -\alpha_s^2 M/9$ . According to the power counting explained above, the c.m. kinetic energies will be neglected. Throughout this paper we set  $\alpha_s = g^2/(4\pi) = 0.4$ .

To calculate rates, we need to average and sum over certain quantum numbers. For convenience, we define

$$|\mathcal{M}|^2 \equiv \sum_{a=1}^8 \sum_{l=1}^3 \sum_{\nu=1}^6 \sum_{\lambda=\pm} |\mathcal{M}_\lambda^{\nu la}|^2 = 2g^2 q^2 |\langle \Psi_{\mathbf{p}_{\text{rel}}} | \mathbf{r} | \psi_{1S} \rangle|^2 \quad (13)$$

for spherically symmetric  $\mathbf{p}_{\text{rel}}$  or  $\mathbf{q}$ . Now the gain and loss terms in the Boltzmann transport equations can be written as

$$\mathcal{C}_+ = \frac{1}{2} \int \frac{d^3 p_1}{(2\pi)^3} \frac{d^3 p_2}{(2\pi)^3} \frac{6}{9} f_c(\mathbf{x}, \mathbf{p}_1, t) f_c(\mathbf{x}, \mathbf{p}_2, t) \frac{d^3 q}{(2\pi)^3 2q} (1 + n_B^{(q)}) \frac{d^3 k_1}{(2\pi)^3} (2\pi)^4 \delta^3(\mathbf{k}_1 + \mathbf{q} - \mathbf{k}_2) \delta(\Delta E) \frac{1}{6} |\mathcal{M}|^2 \quad (14)$$

$$\mathcal{C}_- = \frac{1}{2} \int \frac{d^3 q}{(2\pi)^3 2q} n_B^{(q)} \frac{d^3 p_{\text{rel}}}{(2\pi)^3} \frac{d^3 k_2}{(2\pi)^3} (2\pi)^4 \delta^3(\mathbf{k}_1 + \mathbf{q} - \mathbf{k}_2) \delta(\Delta E) \frac{1}{3} |\mathcal{M}|^2 f_{cc}(\mathbf{x}, \mathbf{p}, t) \equiv \Gamma_d(\mathbf{x}, \mathbf{p}, t) f_{cc}(\mathbf{x}, \mathbf{p}, t). \quad (15)$$

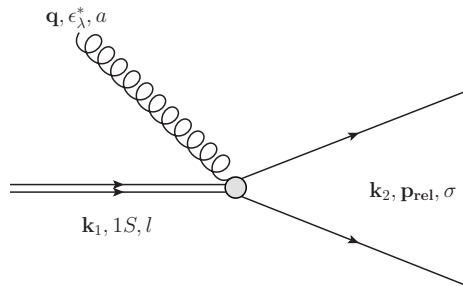


FIG. 1: Transition between bound charm diquark in the anti-triplet and unbound charm quark pair in the sextet by absorbing or emitting an on-shell gluon. Narrow double lines indicate the diquark while widely open double lines represent the unbound pair.

In the second equation we define the dissociation rate of the diquark  $\Gamma_d$ . The factor of  $\frac{1}{6}$  in the formation term is to account for the average over the incoming sextet states while the factor  $\frac{1}{3}$  in the dissociation term is for the average over the incoming anti-triplet. For all pairs of charm quarks, only  $\frac{2}{3}$  of them are in the sextet, which can form a diquark by radiating out a gluon at the order we are working. Formations from unbound anti-triplet pairs happen at higher orders in  $1/M$ .

The scattering amplitude and the rate are calculated in the rest frame of the diquark for dissociation and that of the unbound quark pair for formation, where the pN-RQCD is valid. The Bose distribution of medium gluons  $n_B^{(g)}$  is boosted into the rest frames, respectively. The two frames are not equivalent but since the gluon energy is small compared to  $M$  ( $T \ll M$ ), the difference is suppressed by  $T/M$ . The phase space measure is relativistic for gluons and non-relativistic for charm quarks, which is consistent with our field definitions. The prefactor  $\frac{1}{2}$  avoids double counting in the phase space of two charm quarks.

We test the formation and dissociation rates in a static QGP box with a constant temperature. After evolving for a period long enough, the system of charm quarks and diquarks reaches thermal equilibrium. The equilibrium test is similar to that for heavy quarks and quarkonia in Ref. [9].

To solve the transport equations, an initial condition is needed. Due to the large mass, the charm quark can be thought of being produced from the initial hard scattering in heavy ion collisions, before the QGP is formed. The initial transverse momentum and rapidity distribution from the hard scattering is calculated from FONLL [10] with the nuclear parton distribution function (PDF) EPS09 [11]. The nuclear PDF contains a modification of the proton PDF due to nuclear many-body effects. The FONLL calculation is done with the renormalization and factorization scale  $m_T = \sqrt{M^2 + p_T^2}$ . The number

of charm quarks produced in one collision event is determined by  $\sigma T_{AA}$ , the product of the cross section  $\sigma$  per binary collision calculated in FONLL, and the nuclear thickness function  $T_{AA}$  derived from binary collision models. Here we will focus on collisions with 0–10% centrality, which corresponds to impact parameters from 0 to 5 fm roughly and  $T_{AA} \approx 23$  mb [12].

The initial position of the charm quark produced is sampled using the Trento model [13], a binary collision model. The model assumes the heavy ion collision is a superposition of a number of nucleon-nucleon collisions and calculates the spatial probability distribution where two nucleons from the approaching nuclei scatter. The charm quark production is a short-distance process, implying that its initial position is roughly the same as the location where the two parent nucleons scatter.

Each binary collision also deposits a certain amount of energy and entropy into the system. The Trento model also gives the initial energy and entropy densities. These are then fed into a 2 + 1 dimensional viscous hydrodynamical simulator VISHNew [14, 15], which numerically solves the hydrodynamical equations

$$\partial_\mu T^{\mu\nu} = 0 \quad (16)$$

with the energy-momentum tensor

$$T^{\mu\nu} = eu^\mu u^\nu - (p + \Pi)(g^{\mu\nu} - u^\mu u^\nu) + \pi^{\mu\nu}, \quad (17)$$

$$\Pi = -\zeta \nabla \cdot u, \quad (18)$$

$$\pi^{\mu\nu} = 2\eta \nabla^{(\mu} u^{\nu)} \quad (19)$$

for given initial conditions. Here  $e$  and  $p$  are the local energy density and pressure, and  $u^\mu$  is the local four-velocity of the QGP.  $\Pi$  is the bulk stress with the bulk viscosity  $\zeta$ , and  $\pi^{\mu\nu}$  is the shear stress tensor with the shear viscosity  $\eta$ . Here the angle bracket means traceless symmetrization.

With the initial condition and hydrodynamical background given, we solve the transport equations by test particles Monte Carlo simulations. The hydrodynamical simulation is assumed to start at the co-moving time  $\tau = 0.6$  fm/c. Before this, we assume the charm quarks are just free-streaming without interactions. After  $\tau = 0.6$  fm/c, we consider three types of processes at each time step  $\Delta t = 0.04$  fm/c in the laboratory frame: diffusion, formation and dissociation.

First, for each charm quark and diquark, we determine their thermal scattering rate with medium constituents. The product of the rate and time step  $\Delta t$  gives the scattering probability. Then we use random numbers to determine whether a certain process occurs. If so, we sample the momenta of the incoming medium constituent from a thermal distribution and obtain the momenta of outgoing particles by energy-momentum conservation. Finally, we update both particles' momenta and positions after one time step.

Second, for each diquark, we calculate its dissociation rate and probability within a time step as above. If the diquark is determined to dissociate, we replace it by two unbound charm quarks whose momenta are determined from energy-momentum conservation and whose positions are given by that of the diquark just before the dissociation.

Finally, for each charm quark with position  $\mathbf{y}_i$  and momentum  $\mathbf{k}_i$ , whose neighboring charm quarks have positions  $\mathbf{y}_j$  and momenta  $\mathbf{k}_j$ , we need to determine the di-

quark formation rate by using expression (14). A problem appears, because the two quark distributions should be evaluated at the same position, but the product of two delta functions is ill-defined. We introduce a position dependence of the combination probability by means of a Gaussian function with a width chosen as the diquark Bohr radius  $a_B = \alpha_s M/3$ . This ensures that the combination rate for a widely separated charm quark pair vanishes. The product of local distributions in (14) is thus replaced with

$$f_c(\mathbf{x}, \mathbf{p}_1, t) f_c(\mathbf{x}, \mathbf{p}_2, t) \rightarrow \sum_{i,j} \frac{e^{-(\mathbf{y}_j - \mathbf{y}_i)^2 / 2a_B^2}}{(2\pi a_B^2)^{3/2}} \delta^3\left(\mathbf{x} - \frac{\mathbf{y}_i + \mathbf{y}_j}{2}\right) \delta^3(\mathbf{p}_1 - \mathbf{k}_i) \delta^3(\mathbf{p}_2 - \mathbf{k}_j), \quad (20)$$

where the sum runs over all unbound charm quark pairs. For each charm quark  $i$ , the sum over  $j$  gives the diquark formation rate. If a diquark is formed, we replace the unbound charm quark pair by a diquark whose momentum is determined by momentum conservation and whose position is given by the center-of-mass position of the quark pair as indicated in (20).

When particles reach the hadronization hypersurface determined by the local transition temperature  $T_c \approx 154$  MeV, each diquark combines with a thermal up or down quark to form a doubly charmed baryon. Here we use a simple hadronization model: a massless up or down quark is sampled from a Fermi-Dirac distribution with the temperature  $T_c$ , and its momentum is added to the diquark momentum to determine the baryon momentum. The baryon energy is fixed by the momentum and vacuum mass  $m(\Xi_{cc})$ . In this way, roughly half the diquarks end up as  $\Xi_{cc}^{++}$ . A more realistic hadronization model would include the effect of the baryon wave function on the coalescence probability.

We have simulated 40,000 nuclear collision events. In each event, the initial charm quark momenta is sampled over the range  $p_T \in [0, 30]$  GeV and  $y \in [-8, 8]$ . At the end of each calculation, we accept  $\Xi_{cc}^{++}$  in the kinematic range  $p_T \in [0, 5]$  GeV and  $y \in [-1, 1]$ . The  $p_T$  spectra integrated over this rapidity range are shown in Fig. 2. The yield within this kinematic range is  $N(\Xi_{cc}^{++}) \approx 0.026$  per collision.

So far, we have assumed that the diquark can be formed at any temperature. This cannot be true due to the Debye screening of the attractive color force inside the QGP. To understand the influence of Debye screening on  $\Xi_{cc}^{++}$  production, we repeat the calculation but assume a melting temperature  $T_m = 250$  MeV above which the charm diquark cannot be formed inside the QGP. The yield in the same kinematic range is then reduced to

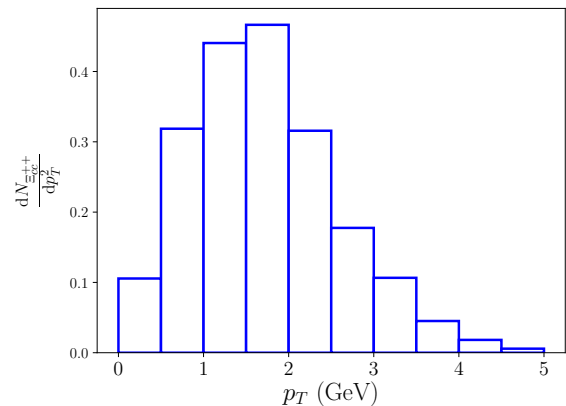


FIG. 2:  $p_T$  spectra of emitted  $\Xi_{cc}^{++}$  integrated over the rapidity window  $-1 \leq y \leq 1$ . The normalization is arbitrary.

$N(\Xi_{cc}^{++}) \approx 0.016$  per collision.

The calculation presented here can be improved in several ways. First, one can include higher-order corrections to the in-medium processes. The in-medium potentials of the diquark can also be made temperature-dependent by performing matching calculations between lattice results of Wilson loops and pNRQCD. Furthermore, one can use more realistic hadronization models. Finally, effects of the initial charm quark momentum distribution modifications from the pre-equilibrium effects could be studied.

In conclusion, we have used Boltzmann transport equations to describe the in-medium formation, dissociation, and transport of charm diquarks. Based on it, we estimate the production rate and  $p_T$  spectra of the doubly charmed baryon  $\Xi_{cc}^{++}$  in central Pb-Pb collision at 2.76 TeV. It will be of great interest if experimental efforts are taken to try to measure  $\Xi_{cc}^{++}$  in heavy ion collisions.

A measurement of the production rate will allow us to extract the melting temperature of the charm diquark in QGP from the above calculation. Furthermore, the melting temperature of heavy diquarks can be studied from finite temperature QCD on a lattice. These experimental and lattice studies will provide valuable information to our understanding of QCD at finite temperature and properties of QGP.

XY acknowledges helpful discussions with Weiyao Ke and Chun Shen and the hospitality of the nuclear theory group at Brookhaven National Laboratory where part of this work was completed. The work is supported from U.S. Department of Energy under Research Grant No. DE-FG02-05ER41367. XY also acknowledges support from Brookhaven National Laboratory.

---

\* Electronic address: xiaojun.yao@duke.edu

† Electronic address: mueller@phy.duke.edu

- [1] R. Aaij *et al.* [LHCb Collaboration], Phys. Rev. Lett. **119**, no. 11, 112001 (2017) [arXiv:1707.01621 [hep-ex]].  
 [2] M. Karliner and J. L. Rosner, Phys. Rev. D **90**, no. 9, 094007 (2014) [arXiv:1408.5877 [hep-ph]].

- [3] P. B. Gossiaux and J. Aichelin, Phys. Rev. C **78**, 014904 (2008) [arXiv:0802.2525 [hep-ph]].  
 [4] P. B. Gossiaux, R. Bierkandt and J. Aichelin, Phys. Rev. C **79**, 044906 (2009) [arXiv:0901.0946 [hep-ph]].  
 [5] J. Uphoff, O. Fochler, Z. Xu and C. Greiner, J. Phys. G **42**, no. 11, 115106 (2015) [arXiv:1408.2964 [hep-ph]].  
 [6] S. Bass, W. Ke and Y. Xu, in preparation.  
 [7] N. Brambilla, A. Vairo and T. Rosch, Phys. Rev. D **72**, 034021 (2005) [hep-ph/0506065].  
 [8] S. Fleming and T. Mehen, Phys. Rev. D **73**, 034502 (2006) [hep-ph/0509313].  
 [9] X. Yao and B. Müller, arXiv:1709.03529 [hep-ph].  
 [10] M. Cacciari, M. Greco and P. Nason, JHEP **9805** (1998) 007 [arXiv:hep-ph/9803400]; M. Cacciari, S. Frixione and P. Nason, JHEP **0103** (2001) 006 [arXiv:hep-ph/0102134].  
 [11] K. J. Eskola, H. Paukkunen and C. A. Salgado, JHEP **0904**, 065 (2009) [arXiv:0902.4154 [hep-ph]].  
 [12] B. Abelev *et al.* [ALICE Collaboration], Phys. Rev. C **88**, no. 4, 044909 (2013) [arXiv:1301.4361 [nucl-ex]].  
 [13] J. S. Moreland, J. E. Bernhard and S. A. Bass, Phys. Rev. C **92**, no. 1, 011901 (2015) [arXiv:1412.4708 [nucl-th]].  
 [14] H. Song and U. W. Heinz, Phys. Rev. C **77**, 064901 (2008) [arXiv:0712.3715 [nucl-th]].  
 [15] C. Shen, Z. Qiu, H. Song, J. Bernhard, S. Bass and U. Heinz, Comput. Phys. Commun. **199**, 61 (2016) [arXiv:1409.8164 [nucl-th]].